Quadruple-Junction Thin-Film Silicon Solar Cells Using Four Different Absorber Materials

Fai Tong Si, Olindo Isabella, Hairen Tan, and Miro Zeman*

We fabricated and studied quadruple-junction wide-gap a-Si:H/narrow-gap a-Si:H/a-SiGe$_x$:H/nc-Si:H thin-film silicon solar cells. It is among the first attempts in thin-film photovoltaics to make a two-terminal solar cell with four different absorber materials. Several tunnel recombination junctions were tested, and the n-SiO$_x$:H/p-SiO$_x$:H structure was proven to be a generic solution for the three pairs of neighboring subcells. The proposed combination of absorbers led to a more reasonable spectral utilization than the counterpart containing two nc-Si:H subcells. Besides, the use of high-mobility transparent conductive oxide and modulated surface texture significantly enhances the total light absorption in the absorber layers. This work paved the way toward high-efficiency quadruple-junction cells, and a practical estimation of the achievable efficiency was given.

1. Introduction

In the quest for higher power conversion efficiency of photovoltaic (PV) devices, the multi-junction solar cell attracts a great deal of research and development. By properly stacking multiple solar cells, each that contains an absorber material with a different bandgap, multi-junction solar cells reduce the thermalization losses and thus, improve the spectral utilization in the power conversion process.

The thin-film silicon solar cell has been established as a highly mature PV technology which exhibits excellent control in module manufacturing over a very large area. In the scope of this PV technology, the efficiency improvement by the multi-junction approach has been well demonstrated up to the triple-junction. The record efficiency of stabilized lab cells is 11.8%,[1] 12.7%,[2] and 14.0%[3] for the single-, double- and triple-junction cells, respectively. The same trend holds true for the record initial efficiency,[4,5] which is up to 16.3% for triple-junction cells. To pursue improvements beyond the triple-junction, several labs have made quadruple-junction (4J) thin-film silicon solar cells with different combinations of absorber materials among hydrogenated amorphous silicon oxide (a-SiO$_x$:H), hydrogenated amorphous silicon (a-Si:H), hydrogenated amorphous silicon germanium (a-SiGe$_x$:H), and hydrogenated nanocrystalline silicon (nc-Si:H).[6–11] So far, an initial efficiency of up to 14.0% has been achieved.[7]

Interestingly, most of the reported 4J thin-film silicon solar cells use the same absorber material, nc-Si:H in their third and fourth subcells. A 4J device structure typically consists of a-Si:H/a-Si:H/nc-Si:H/nc-Si:H absorbers in the four subcells, and the two a-Si:H absorbers can be made to have different bandgaps. While the use of nc-Si:H in more than one subcell is a reasonable choice to mitigate the negative influence of light-induced degradation in devices comprising amorphous absorber materials, it does not promote a better spectral utilization, which is one of the main motives of making multi-junction solar cells. The spectral response of such a 4J cell is exemplified in **Figure 1**a. The third and fourth subcells share the same spectral region of effective absorption. The relatively high-energy photons absorbed in the third subcell do not result in any additional voltage compared to the low-energy ones absorbed in the bottommost counterpart. In order to fulfill a more reasonable spectral utilization in 4J thin-film silicon solar cells, we propose to replace the third absorber with a-SiGe$_x$:H, which has an intermediate bandgap between those of a-Si:H and nc-Si:H. Such configuration or a similar type has recently been reported at conferences by us and another group.[12,13] An optical simulation shows in Figure 1b that such alteration is effective in reducing the spectral overlap. Quantitatively, the overlap can be assessed with the spectral response by the full width at half maximum (FWHM) of the spectral envelope of the overlapping parts. In Figure 1a, such FWHM values for three pairs of neighboring subcells are 99/81/284 nm. In comparison, the FWHM values of 102/76/87 nm exhibit a great improvement for the new structure in Figure 1b.

In this work, we fabricated 4J thin-film silicon solar cells featuring four different abosrber materials – wide-gap (W) a-Si:H, narrow-gap (N) a-Si:H, a-SiGe$_x$:H, and nc-Si:H. Several structures of tunnel recombination junction (TRJ) were examined to find the effective interconnection between the subcells. Optically, the importance of high-mobility transparent conductive oxide (TCO) was highlighted, and modulated surface textured (MST) front electrode was applied in 4J cells for enhanced light absorption.

F. T. Si, O. Isabella, H. Tan, M. Zeman
Photovoltaic Materials and Devices Laboratory, Delft University of Technology, Mekelweg 4, 2628 CD Delft, The Netherlands
E-mail: f.t.si@tudelft.nl

DOI: 10.1002/solr.201700036

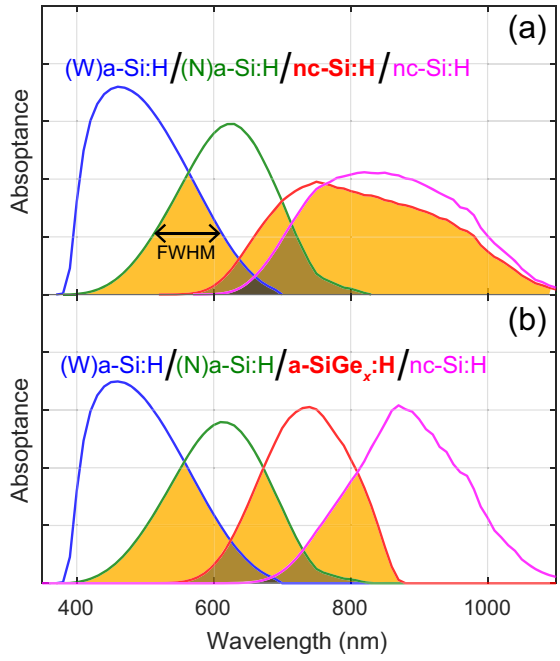

Figure 1. Spectral absorptance of the absorber layers, which represents EQE in case of perfect carrier collection, in 4J thin-film silicon solar cells, given by *GenPro4*[32,33] optical simulations. (a) nc-Si:H and (b) a-SiGe$_x$:H are used in the third subcell of the simulated structures, respectively. Current matching was obtained in the simulations by setting the bottommost nc-Si:H of 3.5 μm thick and other absorber thicknesses unconstrained. The shaded areas indicate the overlapping parts of the photoresponse. (W)a-Si:H and (N)a-Si:H represent a-Si:H with wide and narrow bandgaps, respectively.

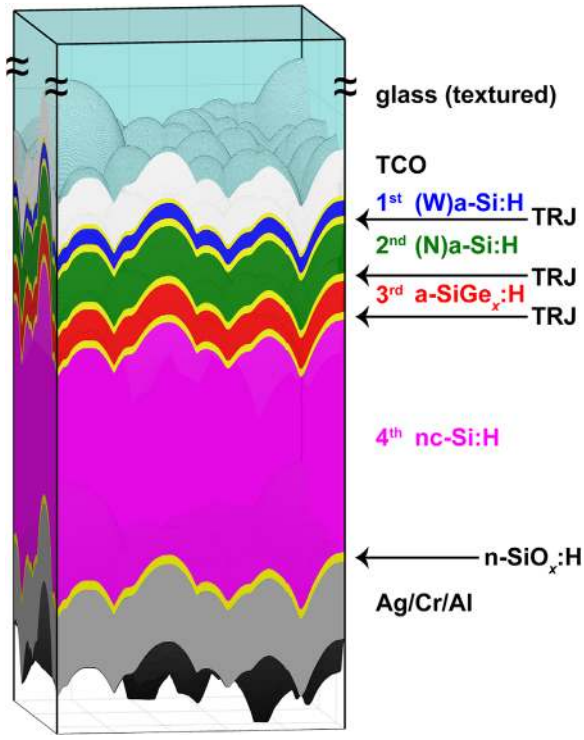

Figure 2. An illustration of the proposed device structure for the 4J (W)a-Si:H/(N)a-Si:H/a-SiGe$_x$:H/nc-Si:H thin-film silicon solar cells. The light enters from the glass side. In our definition, a TRJ includes all doped layers between the two neighboring absorber layers.

2. Experimental

Quadruple-junction (W)a-Si:H/(N)a-Si:H/a-SiGe$_x$:H/nc-Si:H thin-film silicon solar cells were fabricated in superstrate configuration. The device structure is depicted in **Figure 2**. The micro-textured glass substrates were prepared with a chemical etching process which involves an HF/H_2O_2 etchant and an In_2O_3:Sn sacrificial layer.[14] ZnO:Al (AZO) or In_2O_3:H (IOH) was deposited as the front TCO material by radio-frequency magnetron sputtering. In case of the MST substrates, a non-intentionally doped ZnO layer was deposited by low-pressure chemical vapor deposition on micro-textured glass to provide a nanotextured surface.[4] The *p-i-n* junctions of the solar cells were made by plasma-enhanced chemical vapor deposition (PECVD). The optical bandgaps E_{Tauc} of the absorber materials are 1.72, 1.65, 1.42, and 1.12 eV, sequentially. Compared to (N)a-Si:H, the (W)a-Si:H was deposited at a relatively low temperature of 170 °C and the high-pressure regime, and with significant hydrogen dilution.[15] For the intrinsic a-SiGe$_x$:H, linear bandgap grading was applied near the p-i and i-n interfaces.[16] All materials were deposited in the reactor at the radio frequency of 13.56 MHz, except the intrinsic nc-Si:H at the very high frequency of 40.68 MHz. Most of the p- and n-layers were made of mixed-phase hydrogenated silicon oxide (SiO$_x$:H)[17–19] doped with boron and phosphorus, respectively. The metal back reflectors were deposited by thermal (Ag) and e-beam (Cr, Al) evaporation, with a shadow mask defining the cell area as 16 mm^2. The cell isolation was done by removing the materials surrounding the metal pads using anisotropic reactive ion etching. More experimental details regarding the cell fabrication can be found in our previous works.[4,6,15,16]

For the external parameters of the solar cells, the open-circuit voltage (V_{OC}) and fill factor (*FF*) were measured by the illuminated current–voltage (*I–V*) measurement, while the short-circuit current density (J_{SC}) was determined by the external quantum efficiency (EQE) measurement. In the *I–V* measurements, a dual-lamp continuous solar simulator (WACOM WXS-90S-L2, class AAA) was used and the samples were controlled at a stage temperature of 25 °C. Two monocrystalline silicon reference cells, manufactured by and traceable to the Fraunhofer Institute for Solar Energy Systems (ISE), were used to calibrate the two filtered lamps so that the solar simulator provided optimal spectral matching with the AM1.5G solar spectrum and an incident irradiance of 1000 W m^{-2}. The EQE measurements were conducted with an in-house system, in which the light source calibration was done using a silicon photodiode regularly calibrated by Fraunhofer ISE. Bias lights, which were realized by light-emitting diodes (LEDs) with certain emission peaks, were applied so that the subcells not being measured are highly conductive and thus pose a negligible limitation to the measured current. A bias voltage was applied to offset the subcell being measured to its short-circuit condition. The measurement principle is further described in literature.[20,21]

3. Results and Discussion

3.1. Tunnel Recombination Junctions

In two-terminal multi-junction solar cells, the carriers generated in a subcell should either be collected at one of the electrodes, or recombine with the opposite carriers from the neighboring subcell, in the vicinity of the interface between the two subcells. The recombination process is facilitated by tunnel

recombination junctions. To minimize the electrical losses from ineffective recombination, we tested several configurations of TRJ for the three pairs of neighboring subcells in our 4J cell.

Single-junction and dual-junction solar cells were fabricated to resemble the respective parts in the 4J cell. For each pair of neighboring subcells in the 4J cell, TRJs consisting of different material combinations were used in the dual-junction cells while keeping the rest of the structure unchanged. The performance of the TRJs was examined by comparing the V_{OC} of the tandem to the sum of V_{OC} of the two component single-junction cells under AM1.5G illumination. A ΔV_{OC} close to zero is desirable, meaning that the voltages supplied by the subcells can stack up efficiently.

The comparison of the TRJ performance is shown in **Table 1**. Although the use of highly conductive doped nc-Si:H was reported beneficial to forming a good TRJ, its application with a a-Si:H n-layer appears detrimental to the output voltage of the tandem. For the (W)a-Si:H/(N)a-Si:H dual-junction, other tested TRJs involving the use of n-SiO_x:H give similar result, which is a ΔV_{OC} of 32–34 mV. In this comparison, the poor performance of the n-a-Si:H/n-nc-Si:H/p-SiO_x:H TRJ is ascribed to the difference between n-a-Si:H and n-SiO_x:H. The cause is twofold. First, the higher activation energy of 200 mV in n-a-Si:H than that of 80 mV in n-SiO_x:H implies a lower electron concentration and lower recombination rate. Besides, the smaller bandgap of n-a-Si:H means that it is less capable of preventing the holes from passing across the n-layer. Both properties are translated into a worse-performing TRJ. Because of its simplicity and consequently easier control over the optical design, the n-SiO_x:H/p-SiO_x:H TRJ structure is preferred among the tested structures. A similar trend is observed in the (N)a-Si:H/a-$SiGe_x$:H dual-junction, even though in this case the doping level in n-SiO_x:H needs to be adjusted for the optimal performance. It is probably due to the narrower bandgap of p-SiO_x:H used in the a-$SiGe_x$:H subcell. Unfortunately, only one TRJ structure was made and tested for the a-$SiGe_x$:H/nc-Si:H dual-junction. In general, n-SiO_x:H/p-SiO_x:H (with appropriate doping levels) exhibits relatively good performance among the TRJs being studied.

In applying the chosen TRJs, 4J solar cells were fabricated on micro-textured glass substrates coated with as-deposited AZO as the front electrode. The thicknesses of the absorber layers are 85/320/190/3500 nm, respectively. The (N)a-Si:H and a-$SiGe_x$:H were limited to these thicknesses so that the subcells can provide reasonable V_{OC} and FF. The resultant 4J cells exhibit a V_{OC} of 2.789 V and FF of 69.7%. The measured EQE and total absorptance of the device (derived from 1–*R*) are shown in **Figure 3**. The total photocurrent density is 23.0 mA cm^{-2}. In spite of the mismatched photocurrents generated over the four subcells, it is clear that the different bandgaps of the absorbers result in different ending edges of the spectral response of the subcells. The FWHM of the spectral overlap between the third and fourth subcells is 115 nm, a clear improvement from a value of 251 nm for the 4J a-SiO_x:H/(N) a-Si:H/nc-Si:H/nc-Si:H cell reported in our previous work.[6]

Table 1. The V_{OC} losses in dual-junction cells with TRJs formed by different materials.

	ΔV_{OC} (mV)		
TRJ materials	1st/2nd	2nd/3rd	3rd/4th
n-a-Si:H/n-nc-Si:H/p-SiO_x:H	−70	−86	–
n-a-Si:H/n-SiO_x:H/p-SiO_x:H	−34	−63	–
n-SiO_x:H/n-nc-Si:H/p-SiO_x:H	−34	−59	–
n-SiO_x:H/p-SiO_x:H	−32	−67	−45
n^+-SiO_x:H/p-SiO_x:H	−34	−59	–

"1st/2nd" means a dual-junction cell comprising the first and second subcells in the 4J cell, which is (W)a-Si:H/(N)a-Si:H, etc.

3.2. Front TCO

The parasitic absorption in the front TCO layer contributes a significant part to the optical losses in solar cells when the absorber is capable of utilizing the near-infrared light. Therefore, a TCO material with a high carrier mobility is preferred for high-efficiency solar cells because the adequate conductance can be achieved with less free-carrier absorption.

Two 4J solar cells, using different TCOs as the front electrode and with the rest of the structure identical, are compared. The one reported in the previous section uses an AZO layer with a thickness of 1 μm. Another one is with 180 nm of IOH. IOH as a TCO material is well known for its high carrier mobility.[22,23] The IOH produced in our lab has a carrier mobility close to 160 cm^2 V^{-1} s^{-1}) and a carrier concentration around 1.3×10^{20} cm^{-3}, in contrast to a mobility less than 25 cm^2 V^{-1} s^{-1}) and concentration higher than 4×10^{20} cm^{-3} in AZO. The two TCO layers used in our solar cells exhibit similar sheet resistance in the range of 15–20 Ω/□. Figure 3 shows the spectral response of the two 4J cells. On the one hand, the EQE of the cell with IOH shows marginal enhancement in the long wavelengths. It is due to the limited light-scattering

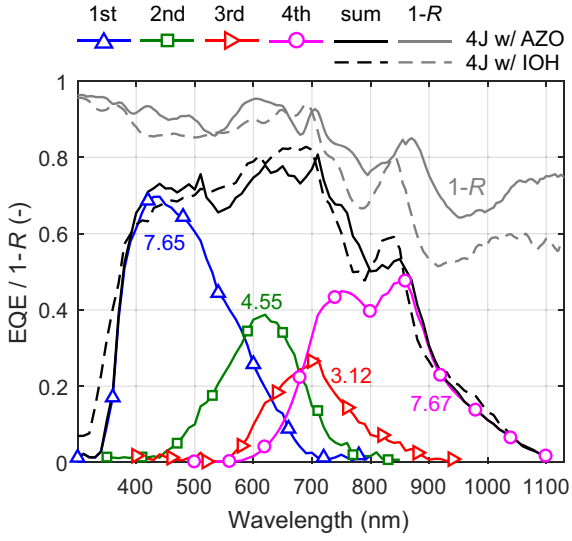

Figure 3. Measured EQE and reflectance spectra of 4J solar cells with either AZO or IOH as the front TCO. While the summed EQE and total absorptance (1 – *R*) are shown for both 4J cells, the EQE of individual subcells is only shown for the cell with AZO. The numbers next to the EQE curves indicate the photocurrent density of the subcells in mA cm^{-2}.

capability of the particular substrates, which contain rather large and smooth micro-texture. Quantitatively, the photocurrent density J_{ph} of the fourth subcell is increased from 7.67 to 7.97 mA cm^{-2}. On the other hand, the more transparent TCO allows more infrared photons to enter the solar cell, as it is evidenced by the total absorptance spectra $(1 - R)$. The 4J cell with IOH, as a whole, absorbs less light in the long wavelengths. Between 700 and 1100 nm, the difference in absorptance is equivalent to a photocurrent of 2.54 mA cm^{-2} under AM1.5G spectrum, and can be ascribed to the additional absorption in AZO. Therefore, by using a high-mobility TCO such as IOH, a greater photocurrent supplied by the infrared light is enabled.

3.3. Enhanced Light Scattering By MST

Effective light scattering always plays an indispensable role in high-efficiency thin-film silicon solar cells, owing to the limited thickness and the low absorption coefficient in near-infrared of the absorbers. With respect to multi-junction cells, the light management is even more demanding as the photogeneration should be evenly distributed among the subcells, and absorption enhancement is needed throughout the whole spectrum between 350 and 1100 nm. It can be seen that the output current of the 4J cells shown in Figure 3 is severely limited by the a-Si:H and a-SiGe$_x$:H subcells. Since there is not much room to further increase the thickness of these absorbers without sacrificing the carrier transportation, enhanced light scattering is crucial for boosting the performance of such devices.

Modulated surface texture has been proven as a powerful tool for enhancing the light absorption throughout a broad spectrum in both thin-film and wafer-based silicon PV technology.[4,14,24–29] Therefore, we implemented MST substrates in 4J solar cells to improve the light scattering. The MST substrate used in this work is the same type as the one reported in our previous work.[4] It comprises, from the surface of light incidence, a micro-textured glass for scattering the low-energy photons, an IOH layer acting as a highly transparent electrode, and a 1 μm of non-intentionally doped ZnO with native nano-texture which facilitates scattering of the short wavelengths and light in-coupling. The micro-texture in the MST has smaller and steeper features than the micro-texture used in the preceding sections, so it should help scatter the light more effectively.[27] The structure of the 4J cell deposited on the MST substrate is the same as before, except the thickness of (W)a-Si:H was slightly reduced to 80 nm to redirect some excess photocurrent to the second subcell. The completed device is presented via scanning electron microscope in **Figure 4**a. In the image, the deposited layers can be clearly distinguished from each other, except for the doped layers which are too thin to be identified. It should also be noted that the rough surface of ZnO is smoothed out after the deposition of the second and third subcells, leaving a favorable surface for depositing high-quality nc-Si:H.[4,14]

The spectral response of the 4J cell on MST substrate and of other reference cells is given in Figure 4b. In relation to the 4J cell on micro-textured substrate with IOH, the MST considerably enhances the light absorption in the 4J cell. As a result of the improved light in-coupling and scattering, the total J_{ph} provided by the three upper subcells increased by 0.91 mA cm^{-2}, while J_{ph} of the bottommost subcell increased by 1.11 mA cm^{-2}, leading to a total J_{ph} of 25.3 mA cm^{-2}, and an overall improvement of 2.02 mA cm^{-2}. The enhancement in spectral response is noticeable over most of the part of the relevant spectrum, which is expected from the advanced design of the MST substrate.

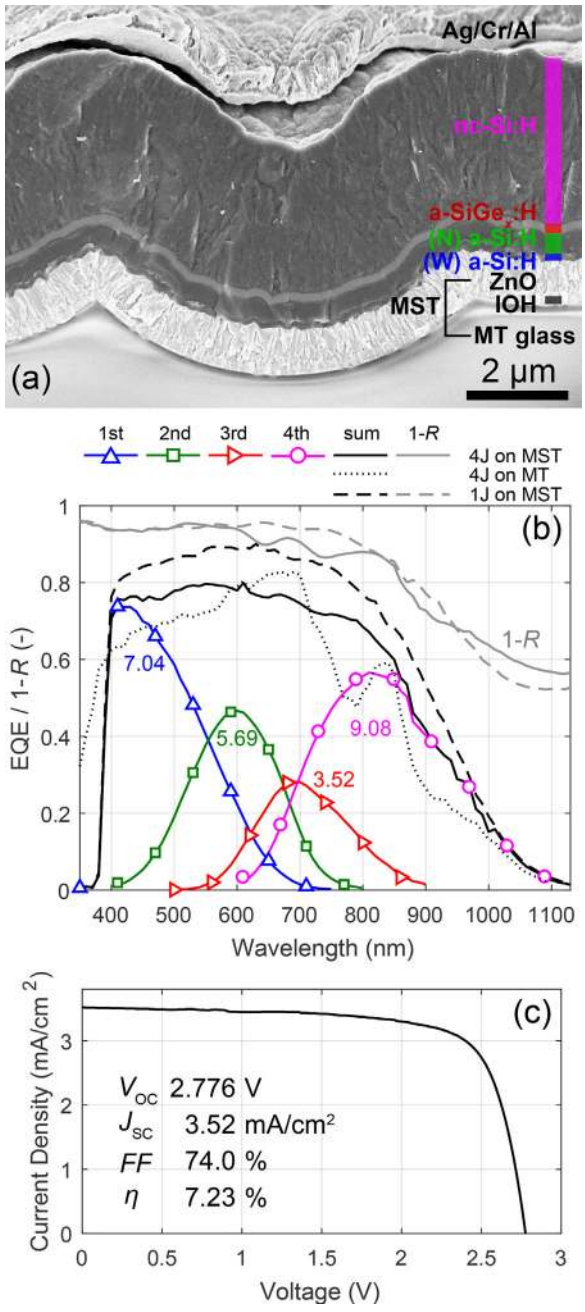

Figure 4. (a) Scanning electron microscope image of the 4J cell fabricated on the MST substrate. The materials and their thicknesses are graphically indicated. (b) Measured EQE and reflectance spectra of the 4J cell on MST substrate. For comparison, the relevant spectra of a single-junction nc-Si:H cell on MST substrate and the 4J cell on micro-textured (MT) substrate with IOH are also plotted. The EQE of the single-junction cell was measured with a negative bias voltage of −3 V to emphasize the optical absorption. (c) *J-V* curve of the best 4J cell on MST substrate. The external parameters indicated in the graph are of the best cell, while the average parameters are reported in the text.

Electrically, the demonstrated 4J cell on MST substrate exhibited an average V_{OC} and FF of 2.769 V and 71.9%, respectively. The *J–V* curve is given in Figure 4c. The reduced V_{OC} compared to that on micro-texture is probably caused by the influence of the rougher surface texture on the thin (W)a-Si:H subcell. Further optimization on material deposition and TRJ design is required to close the gap between the obtained voltage and the ideal one.

3.4. Potential Improvements

Despite the added photocurrent, the J_{SC} of the 4J cell was still limited by the a-SiGe$_x$:H subcell. The first practical solution to tackle the current mismatch is to redistribute the photocurrents among the first, second, and third subcells. By reducing the thicknesses of (W)a-Si:H and (N)a-Si:H absorbers, a J_{ph} of 5.42 mA cm^{-2} in each of these subcells can be approached. Considering the excess photocurrent in the fourth subcell, a thicker n-SiO$_x$:H layer could have been made between the third and fourth subcells to raise the intermediate reflection and thus, make the photocurrent better distributed.[27,30,31] Optical simulations with *GenPro4*[32,33] were performed to examine the effect of intermediate reflectors. By using an n-SiO$_x$:H n-layer in the a-SiGe$_x$:H subcell with a slightly lower refractive index and a thickness of 100 nm in contrast to the original 30 nm, the J_{ph} of the second and third subcells in total can be increased by 1.24 mA cm^{-2}. It can lead to a J_{ph} of 5.83 mA cm^{-2} in each of the three upper subcells. However, the aim of the presented 4J cell was to explore the photocurrent achievable in 4J cells on the MST substrate. An intermediate reflector would lower the total J_{ph} and that of the fourth subcell, so it was not intentionally deployed in this fabricated cell.

To give an outlook on the potential improvement based on this device structure, a single-junction solar cell was fabricated on the MST substrate with the same nc-Si:H absorber thickness of 3.5 μm. The EQE measured at a bias voltage of −3 V is plotted in Figure 4b to demonstrate the optical potential of this MST substrate. The equivalent J_{ph} is 28.9 mA cm^{-2} in the single-junction, and the possible absorption in 4J cells should be even greater considering the larger total thickness of the absorber layers. The difference in EQE between the single-junction and 4J (summed) is ascribed to the extra parasitic absorption in the doped layers, the light escaping the cell from intermediate reflection, and the imperfect carrier collection in the thick amorphous subcells. Should these issues be engineered, a total J_{ph} over 28 mA cm^{-2} in a 4J cell on MST substrate would be feasible. If we take into account the fact that the performance of a-SiGe$_x$:H deteriorates with increased absorber thickness, this restriction reduces the possible J_{SC} to an approximate 6.5 mA cm^{-2}, revealed by another optical simulation using 250 nm a-SiGe$_x$:H (E_{Tauc} 1.41 eV) absorber and intermediate reflector in the third subcell.

Based on the materials and fabrication processes currently available in our lab, we suggest that a well-optimized 4J cell with this structure will exhibit V_{OC} of 3.0 V, J_{SC} of 6.5 mA cm^{-2}, FF higher than 72%, and an initial efficiency of 14.0%. The high V_{OC} was estimated with considerations of the V_{OC} of the corresponding single-junction cells and minor voltage losses at the TRJs. To go further, with state-of-the-art a-SiGe$_x$:H subcell fabrication and process optimization which have been demonstrate in literature,[5,34] we suggest that optimized external parameters with V_{OC} of 3.05 V, J_{SC} of 6.5 mA cm^{-2}, FF of 77%, and an initial efficiency of 15.3% are practically achievable.

4. Conclusions

Quadruple-junction (W)a-Si:H/(N)a-Si:H/a-SiGe$_x$:H/nc-Si:H thin-film silicon solar cells have been realized experimentally. By introducing a a-SiGe$_x$:H subcell, the spectral utilization in 4J cells was improved and the spectral overlap between the subcells was mitigated. Several tunnel recombination junctions were examined and it was found that a simple n-SiO$_x$:H/p-SiO$_x$:H structure delivered a satisfactory outcome for all pairs of neighboring subcells. The use of high-mobility In_2O_3:H instead of ZnO:Al at the front electrode allowed more infrared photons to enter and be utilized by the bottom subcells. Further improvement in light management was achieved by modulated surface textured substrates made of highly transparent TCOs. Its light-scattering and anti-reflection effects significantly increased the photocurrent in the 4J cells. Based upon all exploration done in this work, as well as state-of-the-art technology reported in literature, an initial efficiency of 15.3% should be achievable with the proposed structure provided certain optimization takes place.

Acknowledgements

The authors thank the PV-Lab of IMT, EPFL in Neuchâtel, Switzerland, for the deposition of non-intentionally doped ZnO, which was done during H. Tan's visiting research at EPFL. We also thank Dr. Andrea Illiberi, Johan Blanker, and Ariyanto Wibowo Setia Budhi for developing the in-house deposition process of In_2O_3:H, and Gianluca Limodio for the helpful discussion. This work was supported by the Foundation for Fundamental Research on Matter (FOM), which is part of the Netherlands Organization for Scientific Research (NWO).

Received: February 4, 2017
Revised: March 10, 2017
Published online: March 31, 2017

[1] Sai, H., Maejima, K., Matsui, T., Koida, T., Kondo, M., Nakao, S., Takeuchi, Y., Katayama, H., Yoshida, I., *Jpn. J. Appl. Phys.* **2015**, *54*, 08KB05.
[2] Matsui, T., Bidiville, A., Maejima, K., Sai, H., Koida, T., Suezaki, T., Matsumoto, M., Saito, K., Yoshida, I., Kondo, M., *Appl. Phys. Lett.* **2015**, *106*, 53901.
[3] Sai, H., Matsui, T., Matsubara, K., *Appl. Phys. Lett.* **2016**, *109*, 183506.
[4] Tan, H., Moulin, E., Si, F. T., Schüttauf, J.-W., Stuckelberger, M., Isabella, O., Haug, F.-J., Ballif, C., Zeman, M., Smets, A. H. M., *Prog. Photovoltaics Res. Appl.* **2015**, *23*, 949.
[5] Yan, B., Yue, G., Sivec, L., Yang, J., Guha, S., Jiang, C.-S., *Appl. Phys. Lett.* **2011**, *99*, 113512.
[6] Si, F. T., Santbergen, R., Tan, H., van Swaaij, R. A. C. M. M., Smets, A. H. M., Isabella, O., Zeman, M., *Appl. Phys. Lett* **2014**, *105*, 63902.
[7] Kirner, S., Neubert, S., Schultz, C., Gabriel, O., Stannowski, B., Rech, B., Schlatmann, R., *Jpn. J. Appl. Phys.* **2015**, *54*, 08KB03.

[8] Schüttauf, J.-W., Niesen, B., Löfgren, L., Bonnet-Eymard, M., Stuckelberger, M., Hänni, S., Boccard, M., Bugnon, G., Despeisse, M., Haug, F.-J., Meillaud, F., Ballif, C., *Sol. Energy Mater. Sol. Cells* **2015**, *133*, 163.
[9] Urbain, F., Smirnov, V., Becker, J.-P., Lambertz, A., Yang, F., Ziegler, J., Kaiser, B., Jaegermann, W., Rau, U., Finger, F., *Energy Environ. Sci.* **2016**, *9*, 145.
[10] Urbain, F., Smirnov, V., Becker, J.-P., Lambertz, A., Rau, U., Finger, F., *Sol. Energy Mater. Sol. Cells* **2016**, *145*, 142.
[11] Smirnov, V., Urbain, F., Lambertz, A., Finger, F., *Energy Procedia* **2016**, *102*, 64.
[12] Si, F. T., Isabella, O., Zeman, M., *in 26th Int. Photovolt. Sci. Eng. Conf.* Singapore, **2016**.
[13] Zhang, X., *in OSA Light. Energy Environ. Congr. Opt. Nanostructures Adv. Mater.* Photovoltaics, Leipzig, Germany, **2016**.
[14] Tan, H., Psomadaki, E., Isabella, O., Fischer, M., Babal, P., Vasudevan, R., Zeman, M., Smets, A. H. M., *Appl. Phys. Lett.* **2013**, *103*, 173905.
[15] Fischer, M., Tan, H., Melskens, J., Vasudevan, R., Zeman, M., Smets, A. H. M., *Appl. Phys. Lett.* **2015**, *106*, 43905.
[16] Si, F. T., Isabella, O., Zeman, M., *Sol. Energy Mater. Sol. Cells* **2017**, *163*, 9.
[17] Sichanugrist, P., Yoshida, T., Ichikawa, Y., Sakai, H., *J. Non. Cryst. Solids* **1993**, *164–166*, 1081.
[18] Cuony, P., Alexander, D. T. L., Perez-Wurfl, I., Despeisse, M., Bugnon, G., Boccard, M., Söderström, T., Hessler-Wyser, A., Hébert, C., Ballif, C., *Adv. Mater.* **2012**, *24*, 1182.
[19] Tan, H., Babal, P., Zeman, M., Smets, A. H. M., *Sol. Energy Mater. Sol. Cells* **2015**, *132*, 597.
[20] ASTM E2236-10, Standard Test Methods for Measurement of Electrical Performance and Spectral Response of Nonconcentrator Multijunction Photovoltaic Cells and Modules, **2015**.
[21] Si, F. T., Isabella, O., Zeman, M., *Adv. Energy Mater.* **2016**, *1601930*. https://doi.org/10.1002/aenm.201601930
[22] Koida, T., Fujiwara, H., Kondo, M., *Jpn. J. Appl. Phys.* **2007**, *46*, L685.
[23] Macco, B., Wu, Y., Vanhemel, D., Kessels, W. M. M., *Phys. status solidi – Rapid Res. Lett.* **2014**, *8*, 987.
[24] Oyama, T., Kambe, M., Taneda, N., Masumo, K., Kim, W.-Y., Shibata, A., Kazama, Y., Konagai, M., Takahashi, K., Iida, H., Mishuku, T., Ito, A., Hayashi, Y., Hayashi, Y., Krc, J., Brecl, K., Smole, F., Topic, M., Mizuhashi, M., Gotoh, Y., Adachi, K., Ikeda, T., Sato, K., Hayashi, Y., Wakayama, Y., Adachi, K., Nishimura, H., *in MRS Proc.* Cambridge University Press, Cambridge, United Kingdom, **2008**. pp. K02.
[25] Isabella, O., Moll, F., Krč, J., Zeman, M., *Phys. Status Solidi A* **2010**, *207*, 642.
[26] Hongsingthong, A., Krajangsang, T., Yunaz, I. A., Miyajima, S., Konagai, M., *Appl. Phys. Express* **2010**, *3*, 51102.
[27] Boccard, M., Battaglia, C., Hänni, S., Söderström, K., Escarré, J., Nicolay, S., Meillaud, F., Despeisse, M., Ballif, C., *Nano Lett.* **2012**, *12*, 1344.
[28] Yang, G., van Swaaij, R. A. C. M. M., Tan, H., Isabella, O., Zeman, M., *Sol. Energy Mater. Sol. Cells* **2015**, *133*, 156.
[29] Ingenito, A., Isabella, O., Zeman, M., *Prog. Photovoltaics Res. Appl.* **2015**, *23*, 1649.
[30] Buehlmann, P., Bailat, J., Dominé, D., Billet, A., Meillaud, F., Feltrin, A., Ballif, C., *Appl. Phys. Lett.* **2007**, *91*, 143505.
[31] Boccard, M., Despeisse, M., Escarre, J., Niquille, X., Bugnon, G., Hanni, S., Bonnet-Eymard, M., Meillaud, F., Ballif, C., *IEEE J. Photovoltaics* **2014**, *4*, 1368.
[32] Santbergen, R., van Zolingen, R. J. C., *Sol. Energy Mater. Sol. Cells* **2008**, *92*, 432.
[33] Santbergen, R., Meguro, T., Suezaki, T., Koizumi, G., Yamamoto, K., Zeman, M., *IEEE J. Photovoltaics* **2017**, *1*. https://doi.org/10.1109/JPHOTOV.2017.2669640
[34] B. Liu, L. Bai, Z. Chen, X. Zhang, D. Zhang, J. Ni, Q. Huang, C. Wei, J. Sun, X. Chen, H. Ren, G. Hou, G. Wang, Y. Zhao, *Prog. Photovoltaics Res. Appl.* **2015**, *23*, 1313.

